

## PERTURBATIVE CORRECTIONS TO STAGGERED-FERMION LATTICE OPERATORS

David DANIEL and Stephen N. SHEARD

*Department of Physics, University of Edinburgh, Mayfield Road, Edinburgh EH9 3JZ, Scotland*

Received 9 October 1987

We calculate the relation between staggered bilinear operators on the lattice and their continuum counterparts to one loop, and outline the calculation for four Fermi operators. We apply the Ward identities and symmetries as checks and constraints on the calculation, and give the results in an orthonormal basis of representations of the lattice symmetry group.

### 1. Introduction

QCD has become the accepted theory of low energy non-leptonic physics, but comparison with experiment is not straightforward because of the non-perturbative nature of the observed bound states. Reliable prediction of non-leptonic matrix elements would enable the theory to be tested against currently unexplained features of the experimental data, dominant among which are the  $\Delta I = \frac{1}{2}$  rule in  $K^0 \rightarrow \pi^+ \pi^-$  decays and  $CP$  violation in the kaon system [1]. The lattice regularization of QCD should allow the numerical calculation of these matrix elements with full control over the systematic errors – by the size of the lattice, and the statistical errors – by the size of the statistical sample.

Numerical simulations are being done with both Wilson and staggered fermion formulations. The former method completely resolves the fermion doubling problem, making the choice of lattice operators straightforward, but does not respect chiral symmetry [2]. The latter method retains a continuous  $U(1)_c$  chiral symmetry ensuring chiral behaviour analogous to the continuum, but leaves four doubles for each lattice fermion species, making the choice of lattice operators less obvious [3, 4]. In this paper we deal with staggered fermions. The analogous work has been done for Wilson fermions previously [5, 6].

An essential step in the numerical work is the calculation of the relation between lattice and continuum operators. For sufficiently small lattice spacing this can be done perturbatively. With staggered fermions, the fermion doubles introduce a discrete flavour structure giving more scope for mixing between operators. Further, staggered fermion operators involve link variables where Wilson fermion operators

do not. This results in vertices which vanish in the classical continuum limit, but contribute finite corrections through divergent loop integrals, giving rise to additional mixing and a general suppression of operators associated with link variable fluctuation [7]. However, the radiative corrections to staggered fermions are restricted by Ward identities arising from their residual continuous symmetry.

Both continuum and lattice operators are related to the same tree-level operators by

$$O_i^{\text{cont, latt}} = \left[ \delta_{ij} + \frac{g^2}{(4\pi)^2} Z_{ij}^{\text{cont, latt}} \right] O_j^{\text{tree, level}}, \quad (1)$$

so that they are related to each other by

$$O_i^{\text{cont}} = \left[ \delta_{ij} + \frac{g^2}{(4\pi)^2} Z_{ij} \right] O_j^{\text{latt}}, \quad (2)$$

where we define

$$Z_{ij} = Z_{ij}^{\text{cont}} - Z_{ij}^{\text{latt}}. \quad (3)$$

In the calculation of mesonic matrix elements, two fermion operators are used to create the initial and final meson states, and the effective hamiltonian is an expansion over four-fermion operators. In the  $CP$ -violating kaon system the operator of interest is

$$H_{\text{eff}}^{\Delta S=2} = (\bar{s}\gamma_{\mu L}d)(\bar{s}\gamma_{\mu L}d), \quad (4)$$

where  $\gamma_{\mu L} = \frac{1}{2}\gamma_{\mu}(1 - \gamma_5)$ . The  $\Delta I = \frac{1}{2}$  rule arises from matrix elements of the effective hamiltonian  $\mathcal{H}_{\text{eff}}^{\Delta S=2} = -1$ . After integrating out the heavy fields  $W$ ,  $t$ ,  $b$ ,  $c$  the effective hamiltonian is an expansion over the following six four-fermion operators, characterized by their symmetry under  $SU(2)$  isospin and  $SU(3)$  flavour [8, 9].

$$\begin{aligned} \{8_f, \frac{1}{2}\} \mathcal{O}_1 &= (\bar{d}\gamma_{\mu L}s)(\bar{u}\gamma_{\mu L}u) - (\bar{d}\gamma_{\mu L}u)(\bar{u}\gamma_{\mu L}s), \\ \{8_d, \frac{1}{2}\} \mathcal{O}_2 &= (\bar{d}\gamma_{\mu L}s)(\bar{u}\gamma_{\mu L}u) + (\bar{d}\gamma_{\mu L}u)(\bar{u}\gamma_{\mu L}s) + 2(\bar{d}\gamma_{\mu L}s)[(\bar{d}\gamma_{\mu L}d) + (\bar{s}\gamma_{\mu L}s)], \\ \{27, \frac{1}{2}\} \mathcal{O}_3 &= (\bar{d}\gamma_{\mu L}s)(\bar{u}\gamma_{\mu L}u) + (\bar{d}\gamma_{\mu L}u)(\bar{u}\gamma_{\mu L}s) + (\bar{d}\gamma_{\mu L}s)[2(\bar{d}\gamma_{\mu L}d) - 3(\bar{s}\gamma_{\mu L}s)], \\ \{27, \frac{3}{2}\} \mathcal{O}_4 &= (\bar{d}\gamma_{\mu L}s)(\bar{u}\gamma_{\mu L}u) + (\bar{d}\gamma_{\mu L}u)(\bar{u}\gamma_{\mu L}s) - (\bar{d}\gamma_{\mu L}s)(\bar{d}\gamma_{\mu L}d), \\ \{8, \frac{1}{2}\} \mathcal{O}_5 &= (\bar{d}\gamma_{\mu L}t^I s) \sum_{q=u, d, s} (\bar{q}\gamma_{\mu R}t^I q), \\ \{8, \frac{1}{2}\} \mathcal{O}_6 &= (\bar{d}\gamma_{\mu L}s) \sum_{q=u, d, s} (\bar{q}\gamma_{\mu R}q). \end{aligned} \quad (5)$$

$t^I$  are the hermitian generators of  $SU(3)_{\text{colour}}$  normalised to  $\text{tr}(t^I t^J) = \frac{1}{2}\delta^{IJ}$ .

The content of the paper is organised as follows. In sect. 2 we derive the Feynman rules for two- and four-fermion operators. These are used in sect. 3 to relate two-fermion operators in the continuum and on the lattice. In sect. 4 we discuss the Ward identities and their use as a check on the calculation and a constraint on the results. The results follow in sect. 5. In sect. 6 we outline the situation for four-fermion operators and our conclusions follow.

### 2. Staggered fermions and their Feynman rules

Before proceeding, it will be helpful to give a brief review of staggered fermions and their interpretation as “flavours” of quark in the continuum limit. This will help clarify the notation used later in the paper.

The staggered fermion action is

$$\begin{aligned}
 S = a^4 \sum_x \sum_\mu \frac{1}{2a} \eta_\mu(x) & (\bar{\chi}(x) U_\mu(x) \chi(x+a\mu) - \bar{\chi}(x+a\mu) U_\mu^\dagger(x) \chi(x)) \\
 & + a^4 \sum_x m \bar{\chi}(x) \chi(x), \tag{6}
 \end{aligned}$$

where  $\eta_\mu(x) = (-1)^{x_1 + \dots + x_{\mu-1}}$ . It involves a single-component, anti-commuting field  $\chi$  (for each colour). In the continuum limit, eq. (6) describes four species of Dirac spinor. There are two approaches to identifying these species directly on the lattice, based on the analyses in coordinate and in momentum space.

The coordinate space method starts from the observation that the action is invariant under translations of  $2a$  but not  $a$ . This suggests partitioning the lattice into hypercubes labelled by coordinates  $\{y | y_\mu/2a \in \mathbf{Z}\}$ . Any point on the lattice can then be specified by a hypercube and its position within that hypercube:

$$x = y + aA, \quad A \in \{0, 1\}^d.$$

The staggered fermion field can now be reparameterized as

$$\begin{aligned}
 \Phi_A(y) &= \frac{1}{4} \chi(y + aA), \\
 \bar{\Phi}_A(y) &= \frac{1}{4} \bar{\chi}(y + aA). \tag{7}
 \end{aligned}$$

In the continuum limit the (free) staggered fermion action then takes the form

$$S \sim \sum_{AB} \int d^4y \bar{\Phi}_A(y) \left[ \sum_\mu (\overline{\gamma_\mu \otimes \mathbf{1}})_{AB} \partial_\mu + m (\overline{\mathbf{1} \otimes \mathbf{1}})_{AB} \right] \Phi_B(y).$$

Here the notation [10] is

$$(\overline{\gamma_S \otimes \xi_F})_{AB} = \frac{1}{4} \text{tr}(\gamma_A^\dagger \gamma_S \gamma_B \gamma_F^\dagger), \quad (8)$$

where  $\gamma_A = \gamma_1^{A_1} \gamma_2^{A_2} \gamma_3^{A_3} \gamma_4^{A_4}$ , and is written in such a manner as to suggest the tensor product of a ‘‘spin’’ matrix  $\gamma_S$  and a ‘‘flavour’’ matrix  $\xi_F$ .

This needs some justification. First, it is quite simple to check that the real, orthogonal,  $16 \times 16$  matrices  $\overline{\gamma_\mu \otimes \mathbf{1}}$ ,  $\mu = 1, \dots, 4$  satisfy the Clifford algebra condition

$$\{\overline{\gamma_\mu \otimes \mathbf{1}}, \overline{\gamma_\nu \otimes \mathbf{1}}\} = 2(\overline{\mathbf{1} \otimes \mathbf{1}}) \delta_{\mu\nu},$$

and so generate a faithful representation of it. However there is only one faithful, irreducible representation of the Clifford algebra with dimension 4, namely the Dirac gamma matrices. Therefore the constructed representation must decompose into 4 irreducible representations each equivalent to the gamma matrix representation, and hence there must be a unitary transformation

$$(\overline{\gamma_\mu \otimes \mathbf{1}})_{AB} \rightarrow (\gamma_\mu \otimes \mathbf{1})^{\alpha a, \beta b}, \quad \alpha, a, \beta, b = 1, \dots, 4.$$

The required unitary transformation is a simple Fierz transformation: in general

$$\sum_{AB} (\frac{1}{2} \gamma_A^{\alpha a}) (\overline{\gamma_S \otimes \xi_F})_{AB} (\frac{1}{2} \gamma_B^{* \beta b}) = (\gamma_S \otimes \xi_F)^{\alpha a, \beta b}, \quad (9)$$

where  $\xi_A = \xi_1^{A_1} \dots \xi_4^{A_4}$ ,  $\xi_\mu = \gamma_\mu^*$ . In this way the sixteen-component field  $\Phi_A$  can be identified with four ‘‘flavours’’ of Dirac spinor, labelled by the index  $a = 1, \dots, 4$ .

A very similar procedure can be applied in momentum space. Any momentum  $k \in [-\pi/a, \pi/a]^4$  (the first Brillouin zone) can be written

$$k = p + \frac{\pi}{a} A, \quad p \in \left[ -\frac{\pi}{2a}, \frac{\pi}{2a} \right]^4.$$

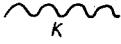
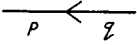
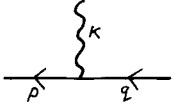
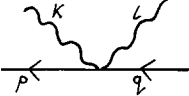
Defining fields

$$\begin{aligned} \tilde{\phi}_A(p) &= \tilde{\chi} \left( p + \frac{\pi}{a} A \right), \\ \bar{\tilde{\phi}}_A(p) &= \tilde{\chi} \left( p + \frac{\pi}{a} A \right), \end{aligned} \quad (10)$$

the free staggered fermion action has the continuum form

$$S \sim \sum_{AB} \int d^4 p \bar{\phi}_A(p) \left[ \sum_{\mu} (\overline{\gamma_\mu \otimes \mathbf{1}})_{AB} \partial_{\mu} + m (\overline{\mathbf{1} \otimes \mathbf{1}})_{AB} \right] \phi_B(p),$$

TABLE 1  
Lattice QCD Feynman rules relevant to the above calculation,  $\bar{\mu} = \sum_1^4 \bar{\mu}$

gluon propagator		$D_{\mu\nu}^{IJ}(k, l) = \frac{\delta^{IJ} \delta_{\mu\nu}}{\sum_{\mu} (4/a^2) \sin^2(a/2) k_{\mu}} \bar{\delta}(k+l)$
quark propagator		$(S^{-1})^{ij}(p, q) = \delta^{ij}(m\bar{\delta}(p+q) + (i/a)\sum_{\mu} \sin ap_{\mu} \bar{\delta}(p+q + (\pi/a)\bar{\mu}))$
vertex		$-ig(t^I)^{ij} \cos a(p + \frac{1}{2}k)_{\mu} \bar{\delta}(p+q+k + (\pi/a)\bar{\mu})$
vertex		$-ag^2 \delta_{\mu\nu} \frac{1}{2} \{t^I, t^J\}^{ij} \sin a(p + \frac{1}{2}k + \frac{1}{2}l)_{\mu} \times \bar{\delta}(p+q+k+l + (\pi/a)\bar{\mu})$

The gluon propagator is in the Feynman gauge.

where another set of spin-flavour matrices appears, related unitarily to the previous  $(\overline{\gamma_S \otimes \xi_F})$  matrices by

$$(\overline{\overline{\gamma_S \otimes \xi_F}})_{AB} = \sum_{CD} \frac{1}{4} (-)^{A \cdot C} (\overline{\gamma_S \otimes \xi_F})_{CD} \frac{1}{4} (-)^{D \cdot B}. \quad (11)$$

The complete equivalence of these two ‘‘flavour interpretations’’ has been discussed in ref. [11]. In the calculations discussed below, it is important to understand the distinction between and yet the equivalence of the two spin-flavour bases  $(\overline{\gamma_S \otimes \xi_F})$  and  $(\overline{\overline{\gamma_S \otimes \xi_F}})$ .

The propagators and vertices associated with the staggered fermion action used in the calculation below are given in table 1. The variables  $p$  and  $q$  cannot be regarded as physical momenta because of the need for some kind of flavour identification in the staggered fermion formulation, in which space-time and spinor properties are intimately connected. It remains to calculate the Feynman rules associated with staggered fermion operators.

The continuum limit of staggered fermion lattice QCD is a continuum QCD with four flavours of mass degenerate quark. In a conventional continuum regularization of such a theory, operators of the form

$$\bar{q}(x) \gamma_S \otimes \xi_F q(x)$$

( $\xi \in$  Lie algebra of  $SU(4)_F$ ) can act as interpolating fields for the physical mesons.

There is a wide choice of lattice transcriptions for the continuum operator  $\bar{q} \gamma_S \otimes \xi_F q$ . The most local operator possible, and one which will be adopted here, is that defined on a single hypercube using the coordinate space-flavour identification

outlined above

$$\mathcal{O}_{\text{SF}}(y) = \sum_{AB} \bar{\Phi}_A(y) (\overline{\gamma_S \otimes \xi_F})_{AB} \mathcal{U}_{AB}(y) \Phi_B(y). \tag{12}$$

Here,  $\mathcal{U}_{AB}(y)$  is a product of gauge links inserted to ensure gauge invariance. To make  $\mathcal{O}_{\text{SF}}$  as symmetric as possible, all shortest paths between  $y + aA$  and  $y + aB$  are averaged over, so that

$$\begin{aligned} \mathcal{U}_{AB}(y) &= \frac{1}{4!} \sum_P U(y + aA, y + aA + \Delta_{P_1}) \\ &\quad \times \cdots \times U(y + aA + \Delta_{P_1} + \Delta_{P_2} + \Delta_{P_3}, y + aB), \\ \Delta_\mu &= a(B - A)_\mu \hat{\mu}. \end{aligned} \tag{13}$$

A last point to make about eq. (12)  $\bar{\Phi}$  and  $\Phi$  need not arise from the same  $\chi$ -field. That is they may correspond to different species of staggered fermion  $\chi_1$  and  $\chi_2$  say.

The presence of gauge links in the definition of such a quasi-local operator means that the vertices for the insertion of an operator in Green functions may have external gluon legs. The vertices required for one-loop calculations are shown in fig. 1. The momentum dependent functions in these vertices are

$$\begin{aligned} M_{\text{SF}}^{(0)}(p, -q) &= \frac{1}{N_f^2} \sum_{AB} e^{iap \cdot A} (\overline{\gamma_S \otimes \xi_F})_{AB} e^{-iaq \cdot B}, \\ M_{\text{SF}}^{(1)\mu}(p, -q; k) &= \frac{1}{N_f^2} \sum_{AB} (B - A)_\mu e^{iap \cdot A} (\overline{\gamma_S \otimes \xi_F})_{AB} e^{-iaq \cdot B} f_{(AB)}^\mu(ak), \\ M_{\text{SF}}^{(2)\mu\nu}(p, -q; k, l) &= \frac{1}{N_f^2} \sum_{AB} (B - A)_\mu (B - A)_\nu \\ &\quad \times e^{iap \cdot A} (\overline{\gamma_S \otimes \xi_F})_{AB} e^{-iaq \cdot B} g_{(AB)}^{\mu\nu}(ak, al), \end{aligned} \tag{14}$$

where  $N_f = 2^{d/2}$  and

$$f_{AB}^\mu(\phi) = \frac{1}{6} e^{i\phi \cdot A} e^{i\phi_\mu (B-A)_\mu / 2} \sum_{\nu \neq \mu} (1 + e^{i\phi_\nu (B-A)_\nu}), \tag{15}$$

$(AB)$  indicates that we have symmetrized on the indices  $A$  and  $B$ . All that is necessary to know about  $g_{AB}^{\mu\nu}(\phi, \psi)$  at one loop is that  $g_{(AB)}^{\mu\mu}(\phi, -\phi) = f_{(AB)}^\mu(\phi)$ .

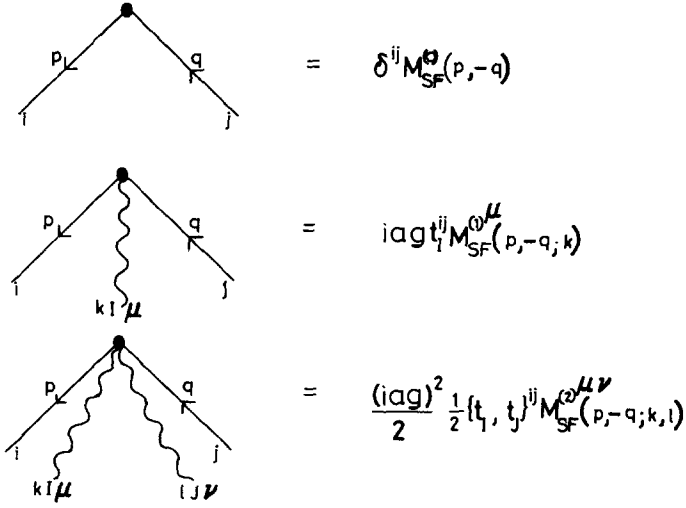


Fig. 1. Vertices for the operator  $\mathcal{O}_{SF}$  required at one loop.

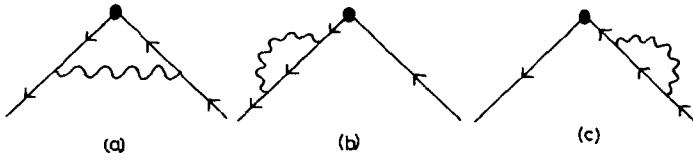


Fig. 2. Continuum diagrams contributing  $\bar{q}\gamma_S \otimes \xi_{Fq}$  at one loop.

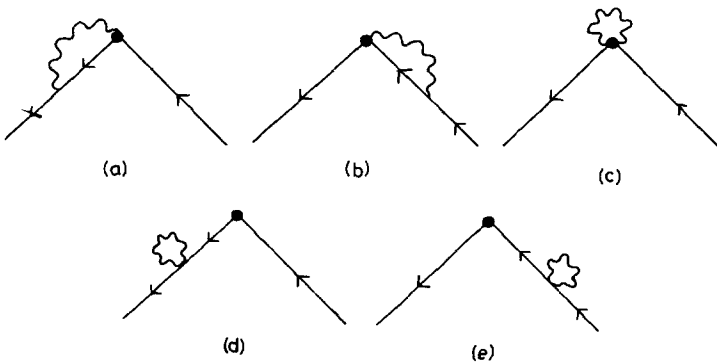


Fig. 3. Additional lattice diagrams contributing to  $\bar{q}\gamma_S \otimes \xi_{Fq}$  at one loop.

At one loop, the perturbative corrections to  $\mathcal{O}_{\text{SF}}$  come from the diagrams of figs. 2 and 3. Remember that only  $\frac{1}{2}$ -times the self-energy diagrams should be included.

A difficulty is immediately apparent: the Feynman rules given above lead, via the relation

$$(-)^{A_\mu} \bar{\delta}^{(a)} \left( p - q + \frac{\pi}{a} (A + B + \bar{\mu}) \right) \rightarrow \bar{\delta}(p - q) \overline{(\gamma_\mu \otimes \mathbf{1})}_{AB}, \quad a(p - q) \rightarrow 0, \tag{16}$$

to spin flavour structure in the momentum space basis, related by eq. (11). An important part of the methodology of staggered fermion loop calculations is to bring everything into a single basis – the  $(\overline{\gamma_S \otimes \xi_F})$  basis.

### 3. Two-quark operators

To renormalize the general two-quark operator  $\bar{q}(x) \gamma_S \otimes \xi_F q(x)$  consider the bare matrix element

$$\langle q(x) \bar{q}(y) \bar{q}(0) \gamma_S \otimes \xi_F q(0) \rangle.$$

There are three momentum-space diagrams contributing at one loop in the continuum. These are shown in fig. 2. The tree-level operator vertex is simply  $\gamma_S \otimes \xi_F$ . Only half of the self-energy diagrams (b) and (c) contribute to the operator, the other half supplying the self-energy to the external states. Using a simple Pauli-Villars cutoff  $Q$ , and an infrared regulating mass  $\kappa$  so that the massless limit of the theory can be taken, the diagrams can be evaluated easily to give

$$(\bar{q} \gamma_S \otimes \xi_F q)^{\text{cont}} = (\bar{q} \gamma_S \otimes \xi_F q)^{\text{tree}} \left[ 1 + \frac{g^2}{(4\pi)^2} C_f (\sigma_S - 1) \ln \frac{Q^2}{\kappa^2} + \text{RI} \right], \tag{17}$$

where  $C_f = (N_c^2 - 1)/2N_c$  is the quadratic Casimir invariant for the fundamental representation of  $\text{SU}(N_c)$  and RI refers to regularization scheme independent integrals which contain all the external momentum dependence. These are finite and will cancel between continuum and lattice schemes so that they need not be considered further.

The coefficient  $\sigma_S$  in eq. (17) is defined by the relation

$$\frac{1}{4} \sum_{\mu\nu} \gamma_\mu \gamma_\nu \gamma_S \gamma_\nu \gamma_\mu = \sigma_S \gamma_S. \tag{18}$$

For  $\gamma_S = \gamma_\mu$  or  $\gamma_{\mu 5}$ , then  $\sigma_S = 1$  so that the vector and axial-vector currents are one-loop finite. This is a consequence of the Ward identities associated with the chiral symmetry of the QCD action.



The important points to note are that, at the massless level in the continuum, perturbative corrections are multiplicative (that is there is no mixing) and independent of the flavour structure. For the specific choice of Pauli-Villars regularization there are no finite corrections (other than the RI term which vanishes at zero external momentum) so that a calculation of the finite corrections to the lattice operators will immediately give the desired connexion between lattice and continuum.

The lattice calculation involves the diagrams of fig. 2 and the additional diagrams of fig. 3. First consider fig. 2a. This is the only divergent diagram apart from the self-energy diagrams whose divergences have been investigated by Golterman and Smit [12]. Taking the external momenta to be  $p + \pi_C/a$  and  $q + \pi_D/a$ ,  $p, q \in [-\pi/2a, \pi/2a]^4$ , and then neglecting the ‘‘physical’’ part of the external momenta ( $p$  and  $q$ ) since this will cancel in the comparison with the continuum result, this diagram has the value

$$\begin{aligned}
 G_{(a)}^2 &= g^2 C_t \int_{-\pi/a}^{\pi/a} \frac{d^4 k}{(2\pi)^4} \frac{d^4 p'}{(2\pi)^4} \frac{d^4 q'}{(2\pi)^4} a^4 B(ak) F(ap') F(aq') \\
 &\times \cos^2 \frac{a}{2} k_\mu \sin ap'_\rho \sin aq'_\sigma N_f^{-2} e^{iap' \cdot A} (\overline{\gamma_S} \otimes \xi_F)_{AB} e^{-iaq' \cdot B} \\
 &\times (-)^{C_\mu} (-)^{D_\rho} \bar{\delta} \left( k - p' + \frac{\pi}{a} (C + \bar{\mu} + \bar{\rho}) \right) \bar{\delta} \left( q' - k + \frac{\pi}{a} (D + \bar{\mu} + \bar{\sigma}) \right),
 \end{aligned}$$

where all repeated indices (except  $C$  and  $D$ ) are summed over, and where

$$B(\phi) = \frac{1}{(a\kappa)^2 + \sum_\mu 4 \sin^2 \frac{1}{2} \phi_\mu}, \tag{19}$$

and

$$F(\phi) = \frac{1}{\sum_\mu \sin^2 \phi_\mu}, \tag{20}$$

$\kappa$  being the infrared-cutoff mass supplied to the gluon.

Now we can extract the spin structure from the constraints by the relations

$$\begin{aligned}
 \bar{\delta} \left( k - p' + \frac{\pi}{a} (C + \bar{\mu} + \bar{\rho}) \right) &= \sum_{C' C''} \bar{\delta} \left( k - p' + \frac{\pi}{a} C'' \right) (\pi_{\bar{\mu}})_{CC'} (\pi_{\bar{\rho}})_{C' C''}, \\
 \bar{\delta} \left( q' - k + \frac{\pi}{a} (D + \bar{\mu} + \bar{\sigma}) \right) &= \sum_{D' D''} \bar{\delta} \left( q' - k + \frac{\pi}{a} D'' \right) (\pi_{\bar{\rho}})_{D'' D'} (\pi_{\bar{\mu}})_{D' D}, \tag{21}
 \end{aligned}$$

where  $(\pi_A)_{BC}$  are defined by

$$\begin{aligned} (\pi_A)_{BC} &= 1 \text{ when } A + B + C = 0 \\ &= 0 \text{ otherwise.} \end{aligned} \quad (22)$$

The integrations over  $p'$  and  $q'$  can now be performed, and the relation  $(-)^{A_\mu}(\pi_{\bar{\mu}})_{AB} = (\overline{\gamma_\mu \otimes \mathbf{1}})_{AB}$  exploited, to give, in terms of the dimensionless loop variable  $\phi = ak$ ,

$$\begin{aligned} G_{(a)}^2 &= g^2 C_t \int_{-\pi}^{\pi} \frac{d^4\phi}{(2\pi)^4} B(\phi) F^2(\phi) \cos^2 \frac{1}{2} \phi_\mu \sin \phi_\rho \sin \phi_\sigma \\ &\times (\overline{\gamma_{\mu\rho} \otimes \mathbf{1}})_{CC'} \frac{1}{N_f} (-)^{C \cdot A} e^{i\phi \cdot A} (\overline{\gamma_S \otimes \xi_F})_{AB} e^{-i\phi \cdot B} \frac{1}{N_f} (-)^{B \cdot D'} (\overline{\gamma_{\sigma\mu} \otimes \mathbf{1}})_{D'D}, \end{aligned} \quad (23)$$

where the notation  $\gamma_{AB} \equiv \gamma_A \gamma_B$  has been used. Note in particular that for the purpose of this chapter  $\gamma_{\mu\nu} = \gamma_\mu \gamma_\nu$ ,  $\forall \mu, \nu$ , so that  $\gamma_{\mu\mu} = \mathbf{1}$ .

If it were not for the  $e^{i\phi \cdot A}$  and  $e^{-i\phi \cdot B}$  terms in this expression, the spin-flavour structure would just be

$$(\overline{\gamma_{\mu\rho S \rho\mu} \otimes \xi_F})_{CD} = \pm (\overline{\gamma_S \otimes \xi_F})_{CD}, \quad (\text{no sum})$$

in which case, then the lattice result would be little different from that in the continuum, with no mixing. In fact there is a thorough mixing of both spin and flavour structures.

To proceed with the evaluation of eq. (23), an expansion of the form

$$e^{i\phi \cdot A} (\overline{\gamma_S \otimes \xi_F})_{AB} e^{-i\phi \cdot B} = \sum_{MN} C_{SF, MN}(\phi) (\overline{\gamma_M \otimes \xi_N})_{AB},$$

which separates the spin-flavour  $(A, B)$  and loop momentum  $(\phi)$  dependence is required. This separation can be achieved with the aid of the identity

$$e^{i\phi \cdot A} (\overline{\gamma_S \otimes \xi_F})_{AB} = \left( \prod_{\mu} e^{i\phi_{\mu}/2} \right) \sum_M E_M(\phi) (\overline{\gamma_{MS} \otimes \xi_{MF}})_{AB}. \quad (24)$$

Here

$$E_M(\phi) = \prod_{\mu} \frac{1}{2} \left( e^{-i\phi_{\mu}/2} + (-)^{\tilde{M}_{\mu}} e^{i\phi_{\mu}/2} \right), \quad (25)$$

where  $\tilde{M}_{\mu} = \sum_{\nu \neq \mu} M_{\nu}$  modulo 2.

Then, using the fact that  $\overline{\gamma_S \otimes \xi_F}$  is a symmetric matrix,

$$e^{i\phi \cdot A} (\overline{\gamma_S \otimes \xi_F})_{AB} e^{-i\phi \cdot B} = \sum_{MN} E_M(\phi) E_N(-\phi) (\overline{\gamma_{MSN} \otimes \xi_{MFN}})_{AB},$$

so that eq. (23) becomes

$$G_{(a)}^2 = g^2 C_f \int_{-\pi}^{\pi} \frac{d^4\phi}{(2\pi)^4} B(\phi) F^2(\phi) \cos^2 \frac{1}{2} \phi_\mu \\ \times \sin \phi_\rho \sin \phi_\sigma E_M(\phi) E_N(-\phi) (\overline{\gamma_{\mu\rho MSN\sigma\mu} \otimes \xi_{MFN}})_{CD}. \quad (26)$$

This integral is logarithmically divergent in the limit  $a\kappa \rightarrow 0$  (see eq. (19)). All of this divergence is located in the  $M = N = (0, 0, 0, 0)$ ,  $\rho = \sigma$  terms of the series, where, in the vicinity of  $\phi = 0$ , the integrand behaves as

$$\frac{1}{4} \frac{1}{\phi^4}.$$

To evaluate this integral numerically, the divergence must be subtracted off before the  $a\kappa \rightarrow 0$  limit is taken. This can be done using the integral  $\mathcal{J}_{0000}(a\kappa)$  defined in appendix A (where the details of such subtractions are discussed).

Once this is done, the final result for fig. 2a is

$$G_{(a)}^2 = \frac{g^2}{(4\pi)^2} C_f \left( \sigma_S (-\ln a^2 \kappa^2 + F_{0000} - \gamma_E) (\overline{\gamma_S \otimes \xi_F})_{CD} \right. \\ \left. + \sum_{\mu\rho\sigma MN} X_{MN}^{\mu,\rho\sigma} (\overline{\gamma_{\mu\rho MSN\sigma\mu} \otimes \xi_{MFN}})_{CD} \right), \quad (27)$$

where  $F_{0000} - \gamma_E = 3.79201(1)$ ,  $\sigma_S$  is defined by eq. (18) and the finite integrals  $X_{MN}^{\mu,\rho\sigma}$  are defined by

$$X_{MN}^{\mu,\rho\sigma} = (4\pi)^2 \int_{-\pi}^{\pi} \frac{d^4\phi}{(2\pi)^4} \left\{ \frac{\cos^2 \frac{1}{2} \phi_\mu \sin \phi_\rho \sin \phi_\sigma E_M(\phi) E_N(-\phi)}{\sum_\alpha 4 \sin^2 \frac{1}{2} \phi_\alpha (\sum_\beta \sin^2 \phi_\beta)^2} \right. \\ \left. - \frac{\delta_{\rho\sigma} \delta_{M,0} \delta_{N,0}}{4 (\sum_\alpha 4 \sin^2 \frac{1}{2} \phi_\alpha)^2} \right\}. \quad (28)$$

Numerical values for these integrals will be discussed below.

Figs. 3a and b are more complicated, but they are finite. The general procedure is the same as above, but because the one gluon vertex of eq. (14) has a more complex momentum dependence, two identities further to eq. (24) are required. These are

$$(B - A)_\mu (\overline{\gamma_S \otimes \xi_F})_{AB} = \frac{1}{2} \left[ \overline{\gamma_{\mu 5 S} \otimes \xi_{\mu 5 F}} - \overline{\gamma_{S \mu 5} \otimes \xi_{F \mu 5}} \right]_{AB}, \quad (29)$$

and

$$e^{i\phi \cdot A} f_{(AB)}^\mu(-\phi) = \frac{1}{12} \sum_{\nu \neq \mu} \sum_{i=1}^4 e^{i(A-B) \cdot \theta_{\mu\nu}^{(i)}}, \quad (30)$$

where

$$\begin{aligned} \theta_{\mu\nu}^{(1)} &= \frac{1}{2} \phi_\mu \hat{\mu}, \\ \theta_{\mu\nu}^{(2)} &= \frac{1}{2} \phi_\mu \hat{\mu} + \phi_\nu \hat{\nu}, \\ \theta_{\mu\nu}^{(3)} &= \phi - \theta_{\mu\nu}^{(1)}, \\ \theta_{\mu\nu}^{(4)} &= \phi - \theta_{\mu\nu}^{(2)}. \end{aligned} \quad (31)$$

Eq. (30) brings figs. 3a and b into a form where eq. (24) can be applied.

At length it is found that

$$\begin{aligned} G_{(a)+(b)}^3 &= \frac{g^2 C_f}{2(4\pi)^2} \sum_{MN\mu\rho} Y_{MN}^{\mu,\rho} \left( \overline{\gamma_{\mu\rho\mu 5 MSN} \otimes \xi_{\mu 5 MFN}} - \overline{\gamma_{\mu\rho MSN\mu 5} \otimes \xi_{MFN\mu 5}} \right. \\ &\quad \left. + \overline{\gamma_{\mu 5 MSN\rho\mu} \otimes \xi_{\mu 5 MFN}} - \overline{\gamma_{MSN\mu 5\rho\mu} \otimes \xi_{MFN\mu 5}} \right)_{CD}, \end{aligned} \quad (32)$$

where the finite lattice integrals  $Y_{MN}^{\mu,\rho}$  are defined by

$$Y_{MN}^{\mu,\rho} = i(4\pi)^2 \int_{-\pi}^{\pi} \frac{d^4\phi}{(2\pi)^4} \frac{\cos^2 \frac{1}{2} \phi_\mu \sin \phi_\rho \frac{1}{12} \sum_{\nu \neq \mu} \sum_i E_M(\theta_{\mu\nu}^{(i)}) E_N(-\theta_{\mu\nu}^{(i)})}{\sum_\alpha 4 \sin^2 \frac{1}{2} \phi_\alpha \sum_\beta \sin^2 \phi_\beta}. \quad (33)$$

The remaining diagrams are much more straightforward:

$$G_{(c)}^3 = -\frac{g^2}{(4\pi)^2} C_{f2} \frac{1}{\mu} \sum_\mu (S - F)_\mu (4\pi)^2 Z_{0000} (\overline{\gamma_S \otimes \xi_F})_{CD}, \quad (34)$$

where  $Z_{0000} = 0.154933(1)$  is defined in appendix A. The evaluation of the self-energy contributions is performed below when Ward identities are considered.

The lattice integrals  $X_{MN}^{\mu,\rho}$  and  $Y_{MN}^{\mu,\rho}$  were evaluated numerically using the Monte Carlo integration package NAGLIB D01 GBF. The results are given in tables 2 and

TABLE 2  
Independent components of the lattice integrals  $X_{MN}^{\mu, \rho\sigma}$

$M$	$X_{MN}^{1,11}$	$X_{MN}^{2,11}$	$X_{MN}^{1,12}$	$X_{MN}^{3,12}$
0000	-0.91366(1)	-0.82302(2)	-0.07291(1)	-0.10407(2)
1000	0.10002(1)	0.02731(1)	0.02731(1)	0.01118(0)
0100	0.05326(0)	0.13439(1)	0.02731(1)	0.01118(0)
0010	0.05326(0)	0.03139(1)	-0.03833(0)	-0.05855(1)
0001	0.05326(0)	0.03139(1)	-0.03833(0)	-0.01629(0)
1100	0.07735(1)	0.04743(0)	-0.07291(1)	-0.10407(2)
1010	0.07735(1)	0.19072(2)	0.03833(0)	0.01629(0)
1001	0.07735(1)	0.19072(2)	0.03833(0)	0.05855(1)
0110	0.13593(1)	0.03833(0)	0.03833(0)	0.01629(0)
0101	0.13593(1)	0.03833(0)	0.03833(0)	0.05855(1)
0011	0.13593(1)	0.16189(2)	-0.02731(1)	-0.01118(0)
0111	0.16355(2)	0.35611(2)	0.07291(1)	0.10407(2)
1011	0.22384(2)	0.07291(1)	0.07291(1)	0.10407(2)
1101	0.22384(2)	0.26284(2)	-0.03833(0)	-0.01629(0)
1110	0.22384(2)	0.26284(2)	-0.03833(0)	-0.05855(1)
1111	0.04103(0)	0.02379(1)	-0.02731(1)	-0.01118(0)

3. The integrals not given can be found using the symmetry properties of  $X$  and  $Y$ :

$$\begin{aligned}
 X_{MN}^{\mu, \rho\sigma} & \quad \text{symmetric on } \rho\sigma \text{ and } MN, \\
 X_{MN}^{\mu, \rho\sigma} = 0 & \quad \text{unless } \tilde{N} + {}_2\tilde{M} = \hat{\rho} + {}_2\hat{\sigma}, \\
 Y_{MN}^{\mu, \rho} & \quad \text{antisymmetric on } MN, \\
 Y_{MN}^{\mu, \rho} = 0 & \quad \text{unless } \tilde{N} + {}_2\tilde{M} = \hat{\rho}. \tag{35}
 \end{aligned}$$

Both integrands are symmetric under permutations of the indices.

As the non-vanishing integrals have even integrands, the integration can be restricted to the domain  $\{0, \pi\}^4$ . The numerical integration converges more quickly for smoother integrand functions obtained by averaging over permutations of the indices, though the calculation of the integrand is then more lengthy. Typically  $10^6$  Monte Carlo hits were required per integral. The accuracy is sufficient for the renormalization results to have errors of order  $10^{-4}$ .

#### 4. Ward identities

As a check on the complex analytic and numerical calculations so far, Ward identities – as always – prove useful. Following from the U(1) invariance of the

TABLE 3  
Independent components of the lattice integral  $Y_{MN}^{\mu,\rho}$

$M$	$Y_{MN}^{1,1}$	$Y_{MN}^{2,1}$
0000	0.85591(1)	0.58329(4)
1000	0.02810(1)	0.00737(1)
0100	0.05716(3)	-0.07906(6)
0010	0.05716(3)	-0.01516(1)
0001	0.05716(3)	-0.01516(1)
1100	0.15787(1)	-0.04284(3)
1010	0.15787(1)	-0.17338(2)
1001	0.15787(1)	-0.17338(2)
0110	0.05716(3)	0.01516(1)
0101	0.05716(3)	0.01516(1)
0011	0.05716(3)	0.07906(2)
0111	0.85591(1)	-0.58329(4)
1011	0.15787(1)	0.04284(3)
1101	0.15787(1)	0.17338(2)
1110	0.15787(1)	0.17338(2)
1111	0.02810(1)	-0.00737(1)

staggered action, there is a set of identities associated with the current

$$J_\mu(x) = \frac{1}{2}\eta_\mu(x) [\bar{\chi}(x)U_\mu(x)\chi(x+a\hat{\mu}) + \bar{\chi}(x+a\hat{\mu})U_\mu^\dagger(x)\chi(x)]. \quad (36)$$

For example the current is conserved

$$\sum_\mu \langle \partial_\mu^{(-)} J_\mu(x) \rangle \equiv \sum_\mu \frac{1}{a} \langle J_\mu(x) - J_\mu(x-a\hat{\mu}) \rangle = 0,$$

which follows from the invariance of the partition function under a local U(1) transformation of the functional integration variables. More interestingly

$$\sum_\mu \langle \partial_\mu^{(-)} J_\mu(x) \bar{\chi}(y)\chi(z) \rangle = \langle \bar{\chi}(y)\chi(z) \rangle [\delta(x-y) - \delta(x-z)], \quad (37)$$

obtained by making a local transformation on  $\langle \bar{\chi}(y)\chi(z) \rangle$ . This has immediate consequences for the perturbative corrections to  $J_\mu$ , since when passing to the renormalized theory by the formal replacements  $\bar{\chi}\chi \rightarrow Z_\chi \bar{\chi}_R \chi_R$  and  $J \rightarrow Z_J J_R$  the wave function renormalizations cancel from either side of the equation, and so  $Z_J$  must be finite. Therefore, all perturbative corrections to  $J$  must be finite.

In fact the Ward identities provide an even stronger constraint than this: perturbative corrections to a conserved current vanish. To see this it is necessary to

derive the Ward identity in terms of 1PI diagrams. At one loop, eq. (37) becomes

$$i \frac{\partial}{\partial p_\lambda} \left\{ \left[ \text{Diagram 1} \right] + \left[ \text{Diagram 2} \right] \right\} = \left[ \text{Diagram 3} \right] + \left[ \text{Diagram 4} \right] + \left[ \text{Diagram 5} \right] + \left[ \text{Diagram 6} \right] \tag{38}$$

so that when self-energy contributions are added to the operator corrections, everything cancels.

What relevance does this discussion to the calculations described above? It so happens that the operator with spin-flavour structure  $\overline{\gamma}_\mu \otimes \mathbf{1}$  is just a superposition of the conserved currents  $J$ : for example

$$\mathcal{O}_{1000,0000}(y) = \sum_{\{A|A_1=0\}} J_\mu(y + aA).$$

So this operator should receive just the same multiplicative corrections as  $J$ , and in particular it should be conserved. This can be checked using the analytic and numerical results derived above. What is required is an explicit verification of the Ward identity eq. (38) for the operator  $\mathcal{O}_{1000,0000}$ .

The cancellation of the self-energy tadpole diagram with that of the operator (eq. (34)) is trivial. To proceed with the other diagrams, an analytic expression for the continuum-like staggered fermion self-energy diagram is required. Calling this graph  $G$ , it turns out that

$$G = \frac{i}{a} g^2 C_f \int_{-\pi}^{\pi} \frac{d^4\phi}{(2\pi)^2} B(\phi) F(\phi + ap) \cos^2(ap + \frac{1}{2}\phi)_\mu \sin(ap + \phi)_\rho \overline{\gamma_{\mu\rho\mu}} \otimes \mathbf{1},$$

where  $p \in [-\pi/2a, \pi/2a]^4$ , and  $B$  and  $F$  were defined in eqs. (19) and (20).

Substituting this expression into the Ward identity eq. (38) and setting external momenta to zero the following relation is found:

$$i \frac{\partial}{\partial p_\lambda} G \Big|_{p=0} = g^2 C_f \left( \int_{-\pi}^{\pi} \frac{d^4\phi}{(2\pi)^4} B(\phi) F^2(\phi) \cos^2 \frac{1}{2} \phi_\mu \sin \phi_\rho \cos \phi_\lambda \overline{\gamma_{\mu\rho\lambda\mu}} \otimes \mathbf{1} + \int_{-\pi}^{\pi} \frac{d^4\phi}{(2\pi)^4} B(\phi) F(\phi) 2 \cos \frac{1}{2} \phi_\lambda \sin \frac{1}{2} \phi_\lambda \sin \phi_\lambda \overline{\gamma_\lambda} \otimes \mathbf{1} \right). \tag{39}$$

The first term corresponds to an integral of the  $X$ -type. It is comparatively straightforward to sum the  $X$  integrals contributing to  $\mathcal{O}_{1000,0000}$  and recover precisely this analytic form.

The second term in eq. (39) corresponds to a  $Y$ -type integral. It is presumably possible to sum the  $Y$  integrals analytically to recover this form. However because of the complexity of the  $Y$  integrals, we perform instead a numerical check. Summing up the numerical estimates of table 3 with the phases appropriate for  $\mathcal{O}_{1000,0000}$  agrees to better than 1% with a direct numerical evaluation of the second term in eq. (39).

This examination of Ward identities provides the easiest way of identifying the contribution of the self-energy diagrams of figs. 2b, c and 3d, e. From each operator it is necessary to subtract off a multiplicative piece exactly big enough to ensure that the vector current  $\mathcal{O}_{1000,0000}$  has vanishing renormalization.

## 5. Results

After including all one-loop terms, the result for a typical two-quark operator is of the form

$$\mathcal{O}^{\text{latt}} = \mathcal{O}^{\text{tree}} \left[ 1 + \frac{g^2}{(4\pi)^2} (\gamma \ln a\kappa + C) \right] + \mathcal{O}^{\text{tree}} \left[ \frac{g^2}{(4\pi)^2} C' \right], \quad (40)$$

where the possibility of mixing has been symbolically included in the  $C'$  term. The one loop anomalous dimension coefficient is  $\gamma = -2C_f(\sigma_S - 1)$ , where  $\sigma_S$  is defined by eq. (18) and  $C_f$  is the group theory factor  $(N_C^2 - 1)/2N_C$ . The results for the finite perturbative corrections  $C, C'$  are given in tables 4 and 5. Errors are of order 1 in the last decimal place. The pseudoscalar, axial vector, and tensor structures not given, are obtained after a transformation,

$$\gamma_A \otimes \xi_B \rightarrow \gamma_A \gamma_5 \otimes \xi_B \xi_5,$$

which leaves all perturbative corrections unchanged. This is the  $U(1)_\epsilon$  transformation on doublet structures.

The notation used is essentially that defined by ref. [13] which runs as follows. The 256 elements  $\gamma_A \otimes \xi_B$  can be thought of as basis vectors for a reducible representation space of the staggered fermion symmetry group given in ref. [13]. This space decomposes into subspaces stable under the group action which can be identified with the irreducible representations of the symmetry group. These are labeled by " $J^{PCU(1)_\epsilon}$ ". The rotation representations are denoted according to the conventions of ref. [14].  $I$  is the identity representation, while Young tableaux are used to label representations of the group of permutations of the axes.  $(j_1, j_2)$  is used to label representations shared with the  $SU(2) \times SU(2)$  covering group of



TABLE 4  
Finite parts of the perturbative corrections to staggered fermion two-quark operators  $\mathcal{O}_{SF}$  with scalar or vector spin structure

Spin-flavour structure	Representation content	Perturbative correction ( $C, C'$ )
$\mathbf{1} \otimes \mathbf{1}$	$I^{++D}$	38.7246
$\mathbf{1} \otimes \xi_\mu$	$I^{--S}, \square^{--S}$	8.1426
$\mathbf{1} \otimes \xi_{\mu\nu}$	$\square^{+-D}, \square^{+D}$	-10.9342
$\mathbf{1} \otimes \xi_{\mu 5}$	$\square^{-+S}, \square^{-+S}$	-25.4759
$\mathbf{1} \otimes \xi_5$	$\square^{++D}$	-38.8560
$\gamma_\mu \otimes \mathbf{1}$	$\left(\frac{1}{2}, \frac{1}{2}\right)^{+-S}$	0.0000
$\gamma_\mu \otimes \xi_5$	$\left(\frac{1}{2}, \frac{1}{2}\right)^{+-S}$	-22.5089
$\left. \begin{array}{l} \gamma_\mu \otimes \xi_\mu \\ \gamma_\mu \otimes \sum_{\nu \neq \mu} \xi_\nu / \sqrt{3} \end{array} \right\}$	$\left(\frac{1}{2}, \frac{1}{2}\right)^{-+D}$	$\begin{pmatrix} 14.7802 & 0.0000 \\ -5.2679 & -10.0407 \end{pmatrix}$
$\left. \begin{array}{l} \gamma_\mu \otimes \xi_{\mu 5} \\ \gamma_\mu \otimes \sum_{\nu \neq \mu} \xi_{\nu 5} / \sqrt{3} \end{array} \right\}$	$\left(\frac{1}{2}, \frac{1}{2}\right)^{-+D}$	$\begin{pmatrix} -34.5001 & 1.1199 \\ 0.0000 & -10.0588 \end{pmatrix}$
$\gamma_1 \otimes (\xi_2 - \xi_3) / \sqrt{2}$	$8^{-+D}$	-10.0407
$\gamma_1 \otimes (\xi_2 - \xi_3) \xi_5 / \sqrt{2}$	$8^{-+D}$	-10.0588
$\gamma_1 \otimes \tau_1 / \sqrt{3}$	$\left(\frac{1}{2}, \frac{1}{2}\right)^{++S}$	3.3960
$\gamma_1 \otimes \tau_{15} / \sqrt{3}$	$\left(\frac{1}{2}, \frac{1}{2}\right)^{++S}$	-22.2421
$\left. \begin{array}{l} \gamma_1 \otimes (\tau_2 - \tau_3) / \sqrt{8} \\ \gamma_1 \otimes (\tau_{25} + \tau_{35} - 2\tau_{45}) / \sqrt{24} \end{array} \right\}$	$8^{++S}$	$\begin{pmatrix} -16.9473 & 9.1710 \\ 11.7452 & -1.8989 \end{pmatrix}$

The notation  $\tau_\mu = \sum_{\nu \neq \mu} \xi_{\mu\nu}$  and  $\tau_{\mu 5} = \tau_\mu \xi_5$  is used.

TABLE 5  
Finite parts of the perturbative corrections to staggered fermion two-quark operators  $\mathcal{O}_{SF}$  with tensor spin structure

Spin-flavour structure	Representation content	Perturbative correction ( $C, C'$ )
$\gamma_{\mu\nu} \otimes \mathbf{1}$	$[(1, 0) \oplus (0, 1)]^{-D}$	-9.9654
$\left. \begin{array}{l} \gamma_{12} \otimes (\xi_1 + \xi_2) / \sqrt{2} \\ \gamma_{12} \otimes (\xi_3 + \xi_4) / \sqrt{2} \end{array} \right\}$	$[(1, 0) \otimes (0, 1)]^{-S}$	$\begin{pmatrix} 0.6818 & 0.0000 \\ 1.3523 & -21.2531 \end{pmatrix}$
$\gamma_{12} \otimes (\xi_1 - \xi_2) / \sqrt{2}$	$6^{--S}$	0.6818
$\gamma_{12} \otimes (\xi_3 - \xi_4) / \sqrt{2}$	$6^{--S}$	-21.2531
$\gamma_{12} \otimes \xi_{12}$	$6^{++D}$	6.8005
$\gamma_{12} \otimes \xi_{34}$	$6^{++D}$	-33.0481
$\gamma_{12} \otimes (\xi_1 + \xi_2)(\xi_3 + \xi_4) / 2$	$[(1, 0) \otimes (0, 1)]^{+D}$	-9.6497
$\gamma_{12} \otimes (\xi_1 - \xi_2)(\xi_3 - \xi_4) / 2$	$[(1, 0) \otimes (0, 1)]^{+D}$	-9.6497
$\gamma_{12} \otimes (\xi_1 - \xi_2)(\xi_3 + \xi_4) / 2$	$6^{++D}$	-9.6497
$\gamma_{12} \otimes (\xi_1 + \xi_2)(\xi_3 - \xi_4) / 2$	$6^{++D}$	-9.6497

SO(4), and finally 6 and 8 refer to additional representations of dimension 6 and 8. The representations  $\bar{R}$  are equivalent to  $R \otimes \begin{smallmatrix} \square \\ \square \end{smallmatrix}$ .

The superscripts  $PCU(1)_\epsilon$  indicate parity under spatial inversions and under “charge conjugation” ( $\gamma_A \otimes \xi_B \rightarrow \gamma_5 \gamma_A^\dagger \gamma_5 \otimes \xi_5 \xi_B^\dagger \xi_5$ ), and also the transformation property under  $U(1)_\epsilon$  transformations ( $S$  for a singlet representation,  $D$  for a doublet). Whilst in four dimensions there is no rotationally invariant reflection, it is still true that the extension of the hypercubic group to include reflections has the effect of doubling all the irreducible representations (irreps) except for the pairs  $(0, 1), (1, 0)$  and  $(\bar{0}, 1), (\bar{1}, 0)$  which merge into larger irreps. With this exception, then, we label the irreps with a parity. The area is covered by ref. [14].

Mixing can occur if the same representation appears more than once in the decomposition. It was found in ref. [13] that the greatest multiplicity of any representation is two. Therefore the largest mixing matrices should be  $2 \times 2$ . Tables 4 and 5 show that this is indeed the case. A simplification follows from the fact that the renormalization constants for  $\gamma_A \otimes \xi_B$  and for  $\gamma_A \gamma_5 \otimes \xi_B \xi_5$  are the same. This is required only for doublet representations of  $U(1)_\epsilon$  (where these two structures are then transformed into one another) but proves to be the case for all spin-flavour structures. The  $U(1)_\epsilon$  transformation maps representation  $R$  of  $W^4$  onto  $R \otimes \begin{smallmatrix} \square \\ \square \end{smallmatrix}$ . In addition the charge conjugation parity may be reversed. The subject is covered in ref. [13].

In case tables 4 and 5 appear to daunting, the representation content can be almost completely ignored. It is included only for comparison with ref. [13]. The column headed “spin-flavour structure” contains a typical normalized basis vector for that representation. The full representation space can be generated from it by the group action.

To explain the use of the tables, consider a fairly complicated example which includes mixing:  $\gamma_\mu \otimes \xi_\nu$ . The anomalous dimension vanishes because this vector current is the lattice analogue of a conserved continuum vector current. For  $\mu = \nu$ , there is no mixing and

$$(\gamma_\mu \otimes \xi_\mu)^{\text{latt}} = (\gamma_\mu \otimes \xi_\mu)^{\text{tree}} \left[ 1 + \frac{g^2 C_f}{(4\pi)^2} C \right], \tag{41}$$

where  $C = 14.7802$  which for  $g \sim 1$  amounts to a 10% enhancement of the lattice operator above the Pauli-Villars operator. In fact, at zero external momentum, this operator has an additional symmetry – that of unit shifts – since it involves no link operators. This symmetry forbids mixing with operators such as  $\gamma_\mu \otimes \xi_\nu$  which do not have it. It does not, however prevent  $\gamma_\mu \otimes \xi_\nu$  mixing into it, so the mixing matrix must be lower triangular. For  $\mu \neq \nu$  there is mixing. Then

$$(\gamma_\mu \otimes \xi_\nu)^{\text{latt}} = (\gamma_\mu \otimes \xi_\nu)^{\text{tree}} \left[ 1 + \frac{g^2 C_f}{(4\pi)^2} C \right] + (\gamma_\mu \otimes \xi_\mu)^{\text{tree}} \left[ \frac{g^2 C_f}{(4\pi)^2} C' \right], \tag{42}$$

where  $C = -10.0407$  and  $C' = -5.2679/\sqrt{3} = -3.0414$ . This follows by expressing  $\gamma_\mu \otimes \xi_\nu$  in terms of the basis vectors

$$\gamma_\mu \otimes \sum_{\nu \neq \mu} \xi_\nu / \sqrt{3}, \quad \gamma_\mu \otimes (\xi_\kappa - \xi_\lambda) / \sqrt{2}.$$

So these two link operators are suppressed by about 10% with respect to their continuum counterparts, as well as having a small mixing with the local operator  $\gamma_\mu \otimes \xi_\mu$ . Suppression of multilink operators can be understood intuitively as being due to the fluctuations of the inserted gauge links. The major contribution comes from diagrams with gluon tadpoles.

### 6. Four-quark operators

In this section we follow the corresponding calculation for four-Fermi operators appropriate to the effective hamiltonians  $\mathcal{H}_{\text{eff}}^{\Delta S=-1}$  and  $\mathcal{H}_{\text{eff}}^{\Delta S=-2}$ . The mixing is restricted by the same symmetries as in the two-quark case, but there are  $16^4$  rather than  $16^2$  spin-flavour structures. Thus, the mixing matrices will be much larger. The spin structure of interest is  $\gamma_{\mu L} \otimes \gamma_{\mu L}$ . Using discrete flavour  $\xi_5 \otimes \xi_5$  to make direct contact with the Ward identities [15] the overall symmetries are  $I^{++S}$  and  $I^{-+S}$ . Alternatively, using discrete flavours  $\xi_{\mu L} \otimes \xi_{\mu L}$  to project out the spin structure [16] the symmetries used are  $I^{++D}$  and  $\prod^{--D}$ . We are aiming to calculate the mixing matrices for these structures.

To set the scene for the lattice calculation, first consider the calculation in the continuum. The presentation follows that of Altarelli et al. [17] (who extended the calculation to two loops), but uses the simple cutoff regulator used throughout this paper.

Consider the two-operators

$$\begin{aligned} \mathcal{O}_{LL} &= \sum_{\mu} (\bar{q}_1 \gamma_{\mu L} q_2) (\bar{q}_3 \gamma_{\mu L} q_4), \\ \mathcal{O}_{LR} &= \sum_{\mu} (\bar{q}_1 \gamma_{\mu L} q_2) (\bar{q}_3 \gamma_{\mu R} q_4), \end{aligned} \tag{43}$$

where  $\gamma_{L,R} = \frac{1}{2} \gamma_\mu (\mathbf{1} \mp \gamma_5)$ .  $q_{1,\dots,4}$  may be different flavours or not. There are six 1PI one-loop diagrams which correct the operator. These fall in pairs into the three classes shown in fig. 4. In addition the four obvious self-energy diagrams have to be included.

Figs. 4b and c lead to mixing with operators with a different colour structure:

$$\sum_{\mu I} (\bar{q}_1 \gamma_{\mu L} t^I q_2) (\bar{q}_3 \gamma_{\mu L,R} t^I q_4).$$

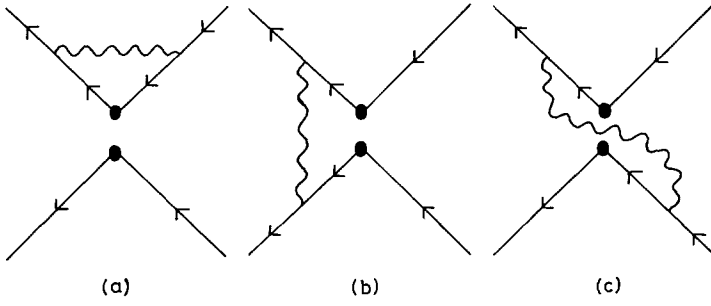


Fig. 4. One-loop graphs contributing to four-quark operators in the continuum.

The crucial difference between diagrams (b) and (c), and diagram (a) is the exchange of a gluon between the fermion lines. For this reason it is sensible to use a basis of Fierz symmetric operators. For  $\mathcal{O}_{LL}$ , the appropriate combinations are

$$\mathcal{O}_{\pm} = \left( \frac{N_C \pm 1}{2N_C} \right) \sum_{\mu} (\bar{q}_1 \gamma_{\mu L} q_2) (\bar{q}_3 \gamma_{\mu L} q_4) \pm \sum_{\mu l} (\bar{q}_1 \gamma_{\mu L} t^l q_2) (\bar{q}_3 \gamma_{\mu L} t^l q_4), \quad (44)$$

which are Fierz symmetric in the sense that

$$\mathcal{O}_{\pm}^{1234} \rightarrow \pm \mathcal{O}_{\pm}^{1432}$$

under the joint application of the Fierz identity and the colour algebra identities

$$\begin{aligned} \delta^{ij} \delta^{kl} &= \frac{1}{N_C} \delta^{il} \delta^{kj} + 2 \sum_I t_I^{ij} t_I^{kl}, \\ \sum_I t_I^{ij} t_I^{kl} &= \frac{1}{N_C} \left( \frac{N_C^2 - 1}{2N_C} \right) \delta^{il} \delta^{kj} - \frac{1}{N_C} \sum_I t_I^{il} t_I^{kj}. \end{aligned} \quad (45)$$

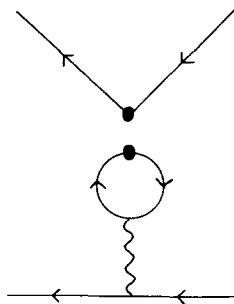


Fig. 5. A penguin graph contributing to the operator  $(\bar{q}_1 q_2)(\bar{q}_3 q_3)$  at one loop.

The superscripts 1234 and 1432 refer to the ordering of the quark fields  $q_i$  in the four-quark operator.

At zero external momenta the result of evaluating all diagrams (including self-energy ones) is

$$\mathcal{O}_{\pm}^{\text{cont}} = \mathcal{O}_{\pm}^{\text{tree}} \left[ 1 - \frac{g^2}{(4\pi)^2} \gamma_{\pm} \ln \frac{Q}{\kappa} \right], \tag{46}$$

where the anomalous dimensions are  $\gamma_{\pm} = \pm 6((N_c \mp 1)/N_c)$ .

In this analysis penguin-type interactions have been neglected. These arise in operators of the form  $(\bar{q}_1 q_2)(\bar{q}_3 q_3)$  which at one loop get corrections from diagrams like that of fig. 5. Such diagrams have recently been studied both in the continuum and on the lattice using Wilson fermions by Bernard et al. [18].

The general four-quark operator is just the product of two-quark operators

$$\mathcal{O}_{SF, S'F'} = \mathcal{O}_{SF} \mathcal{O}_{S'F'}. \tag{47}$$

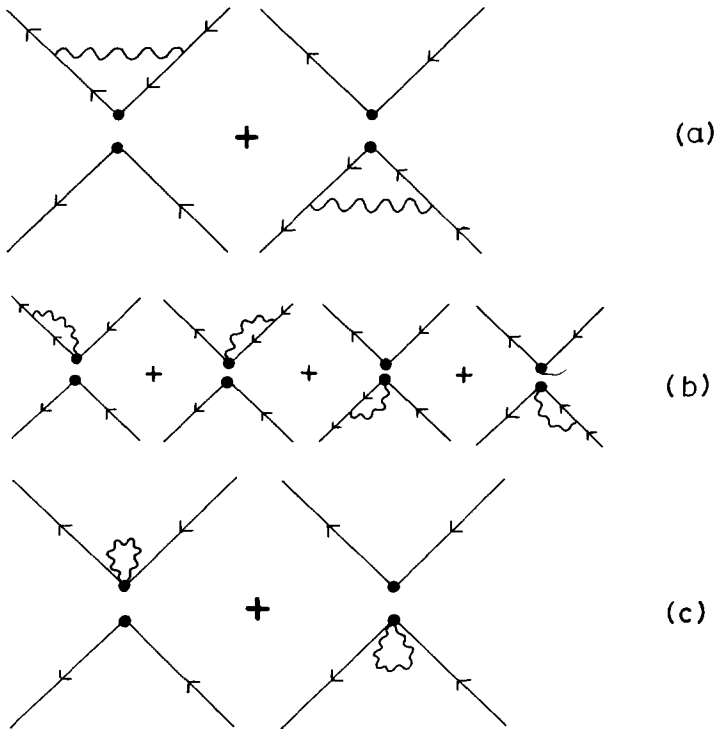


Fig. 6. Diagrams of colour structure  $\mathbf{1} \otimes \mathbf{1}$  contributing at one loop to the staggered fermion four-quark operator  $\mathcal{O}_{SF, S'F'}$ .

Similarly the Feynman rules for four-quark operators are obtained as products of the two quark vertices of fig. 1 and eq. (14).

Operators with the colour structure  $\sum_l t_l^{ij} t_l^{kl}$  arise on the lattice just as they did in the continuum. Their perturbative corrections are found easily from the results presented here by applying eq. (45).

The one-loop corrections to four-quark operators fall into two groups, shown in figs. 6 and 7, the latter having colour structure arising from the exchange of a gluon between the fermion lines. There are 17 1PI diagrams shown, and an additional 8 self-energy diagrams which contribute trivially. The diagrams fall into six classes which are considered separately.

The diagrams in fig. 6 factorize into two two-quark diagrams, so there is no work to be done. The results are

$$G_{(a)}^6 = \frac{g^2}{(4\pi)^2} C_f \left( 2\sigma_S (-\ln a^2 \kappa^2 + F_{0000} - \gamma_E) (\overline{\gamma_S \otimes \xi_F})_{CD} (\overline{\gamma_{S'} \otimes \xi_{F'}})_{C'D'} \right. \\ \left. + \sum_{\mu\rho\sigma MN} X_{MN}^{\mu,\rho\sigma} \left[ (\overline{\gamma_{\mu\rho MSN\sigma\mu} \otimes \xi_{MFN}}) (\overline{\gamma_{S'} \otimes \xi_{F'}}) + (\overline{\gamma_S \otimes \xi_F}) (\overline{\gamma_{\mu\rho MS'N\sigma\mu} \otimes \xi_{MF'N}}) \right] \right), \quad (48)$$

$$G_{(b)}^6 = \frac{g^2 C_f}{2(4\pi)^2} \sum_{MN\mu\rho} Y_{MN}^{\mu,\rho} \\ \times \left\{ \left[ 1 + (-)^{S_\mu + S_\rho} \right] (S'_\mu + 2F'_\mu) (\overline{\gamma_{\rho S MSN} \otimes \xi_{\mu S MFN}}) (\overline{\gamma_{S'} \otimes \xi_{F'}}) \right. \\ \left. + (S_\mu + 2F_\mu) \left[ 1 + (-)^{S'_\mu + S'_\rho} \right] (\overline{\gamma_S \otimes \xi_F}) (\overline{\gamma_{\rho S MS'N} \otimes \xi_{\mu S MF'N}}) \right\}, \quad (49)$$

$$G_{(c)}^6 = -\frac{g^2 C_f}{(4\pi)^2} \left[ \frac{1}{2} \sum_\nu (S - F)_\nu^2 (4\pi)^2 Z_{0000} \right] (\overline{\gamma_S \otimes \xi_F}) (\overline{\gamma_{S'} \otimes \xi_{F'}}). \quad (50)$$

The colour structure is  $\mathbf{1} \otimes \mathbf{1}$ . The multiplicative corrections for  $\mathcal{O}_{SF, S'F'}$  are simply the sum of the two fermion values for  $\mathcal{O}_{SF}$  and  $\mathcal{O}_{S'F'}$ , tables 4 and 5. Mixing corrections from these graphs are easily found from the tables by a change of normalization.

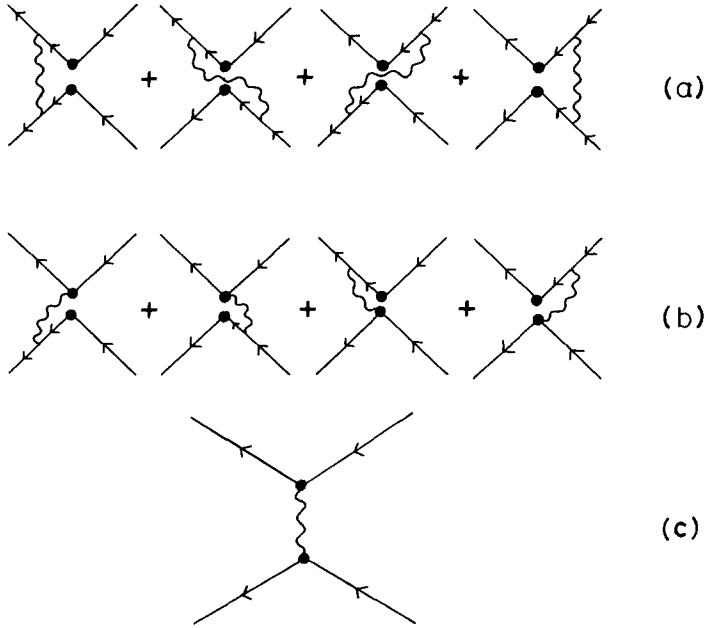


Fig. 7. Diagrams of colour structure  $t_I \otimes t_I$  contributing at one loop to the staggered fermion four-quark operator  $\mathcal{O}_{SF, S'F'}$ .

The colour structure of the diagrams in fig. 7 is  $t_I \otimes t_I$ . The diagrams in class (a) may be expressed in terms of the numerical integrals  $X_{MN}^{\mu, \rho \sigma}$ , but those in classes (b) and (c) require new types of finite lattice integral,  $U_{LMN}^{\mu, \rho}$  and  $V_{KLMN}^{\mu}$  defined by

$$\begin{aligned}
 U_{LMN}^{\mu, \rho} &= i(4\pi)^2 \int_{-\pi}^{\pi} \frac{d^4\phi}{(2\pi)^4} B(\phi) F(\phi) \cos^2 \frac{1}{2} \phi_{\mu} \sin \phi_{\rho} \\
 &\times \frac{1}{12} \sum_{\nu \neq \mu} \sum_i E_L(\theta_{\mu\nu}^{(i)}) E_M(\phi - \theta_{\mu\nu}^{(i)}) E_N(-\phi),
 \end{aligned}
 \tag{51}$$

$$\begin{aligned}
 V_{KLMN}^{\mu} &= (4\pi)^2 \int_{-\pi}^{\pi} \frac{d^4\phi}{(2\pi)^4} B(\phi)^{\frac{1}{12}} \sum_{\nu \neq \mu, i} E_K(\theta_{\mu\nu}^{(i)}) E_L(\phi - \theta_{\mu\nu}^{(i)}) \\
 &\times \frac{1}{12} \sum_{\lambda \neq \mu, j} E_M(-\theta_{\mu\lambda}^{(j)}) E_N(\theta_{\mu\lambda}^{(j)} - \phi).
 \end{aligned}
 \tag{52}$$

The results for these three classes are as follows:

$$G_{(a)}^7 = -\frac{g^2}{(4\pi)^2} \sum_{MN\mu\rho\sigma} X_{MN}^{\mu,\rho\sigma} \left[ \overline{(\gamma_{SM\rho\mu} \otimes \xi_{FN})} - \overline{(\gamma_{\mu\rho MS} \otimes \xi_{MF})} \right] \\ \times \left[ \overline{(\gamma_{S'M\sigma\mu} \otimes \xi_{F'N})} - \overline{(\gamma_{\mu\sigma MS'} \otimes \xi_{MF'})} \right], \quad (53)$$

$$G_{(b)}^7 = -\frac{g^2}{(4\pi)^2} \sum_{LMN\mu\rho} U_{LMN}^{\mu,\rho} \quad (54)$$

$$\times \left\{ (S_\mu + {}_2F_\mu) \overline{(\gamma_{\mu 5 LSM} \otimes \xi_{\mu 5 LFM})} \left[ \overline{(\gamma_{S'N\rho\mu} \otimes \xi_{F'N})} - \overline{(\gamma_{\mu\rho NS'} \otimes \xi_{NF'})} \right] \right. \quad (55)$$

$$\left. + (S'_\mu + {}_2F'_\mu) \left[ \overline{(\gamma_{SN\rho\mu} \otimes \xi_{FN})} - \overline{(\gamma_{\mu\rho NS} \otimes \xi_{NF})} \right] \overline{(\gamma_{\mu 5 LS'M} \otimes \xi_{\mu 5 LF'M})} \right\}, \quad (56)$$

$$G_{(c)}^7 = -\frac{g^2}{(4\pi)^2} \sum_{KLMN\mu} V_{KLMN}^\mu (S_\mu + {}_2F_\mu) (S'_\mu + {}_2F'_\mu) \overline{(\gamma_S \otimes \xi_F)} \overline{(\gamma_{S'} \otimes \xi_{F'})}. \quad (57)$$

These results are not connected to the two-fermion results and require a separate calculation.

## 7. Conclusion and discussion

We have calculated the connection at one loop between staggered bilinear lattice operators and their continuum counterparts. Whilst the symmetries of these operators are sufficient to ensure the correct meson states are excited in quenched LQCD mass calculations, where the discrete flavour is not interpreted as physical, for dynamical LQCD calculations we must identify the discrete flavours as physical so we need to know the rotation of discrete flavour between lattice and continuum. Further, multiplicative corrections will affect the matrix elements in which these operators are used to excite meson states.

The connection is much more important for four-quark operators where the multiplicity of the representations is much greater. The dominant effect we find is the suppression of operators due to fluctuation of the link variables, arising from the tadpole diagrams, fig. 3c. There is a suppression of approximately 10% at  $g \sim 1$  for each link variable involved. Four-quark operators involve up to 8 link variables, giving a suppression of up to 57% at  $g \sim 1$ . However, the contributions from other graphs, and the mixing in particular produce less than 10% effects at one loop. This is encouraging, as we can sum the tadpole diagrams to all orders to effect only a suppression of the vertices in fig. 1. Then the remaining one-loop effects will be below 10% suggesting that higher order terms can be safely neglected. We have not



included penguin diagrams, fig. 5 which Bernard et al. found to be a small effect for Wilson fermion operators [19]. Nor have we included mixing of four quark operators with two-quark operators. The subtraction of these by coupling expansion is delicate [20] and we chose instead to use chiral perturbation theory [15, 16]. In either case such mixings do not affect the coefficients we are calculating.

D.D. wishes to acknowledge the support of the SERC. S.N.S. is funded by the SERC and Fegs Ltd.

## Appendix

### SOME INTEGRALS IN LATTICE WEAK COUPLING PERTURBATION THEORY

A typical integral arising in lattice perturbation theory at one loop is

$$\mathcal{I}(a\{p\}, a\kappa) = \int_{-\pi}^{\pi} \frac{d^4\phi}{(2\pi)^4} f(\phi, a\{p\}, a\kappa), \quad (\text{A.1})$$

where  $\phi/a$  is the loop-momentum, so that  $\phi$  is dimensionless. The lattice spacing  $a$  regulates ultraviolet divergences and  $\kappa$  is the gluon mass introduced to regulate infrared divergences. Two classes of integral occur in the text: those which are finite as  $a\kappa \rightarrow 0$  and those which diverge logarithmically.

The only finite integral needed is

$$Z_{0000} = \int_{-\pi}^{\pi} \frac{d^4\phi}{(2\pi)^4} \frac{1}{\sum_{\mu} 4 \sin^2 \frac{1}{2} \phi_{\mu}} = 0.154933(1), \quad (\text{A.2})$$

which was introduced in ref. [21]. This arises from a closed gluon loop and is purely a lattice artifact. Characteristic of this fact is the absence of external momentum dependence.

Logarithmic divergences can be conveniently isolated by Taylor expansion since

$$\bar{\mathcal{I}}\left(\frac{\{p\}}{\kappa}\right) = \lim_{a\kappa \rightarrow 0} (\mathcal{I}(a\{p\}, a\kappa) - \mathcal{I}(0, a\kappa)) \quad (\text{A.3})$$

is finite *and* (ultraviolet) regulator-independent. Attention then centres on  $\mathcal{I}(0, a\kappa)$  which can be parameterized as

$$\mathcal{I}(0, a\kappa) = \frac{1}{(4\pi)^2} [\gamma \ln a\kappa + C] + \mathcal{O}(a\kappa), \quad (\text{A.4})$$

where  $\gamma$  and  $C$  are finite constants.  $\gamma$  is independent of the regularization scheme (it

contributes to a one-loop anomalous dimension).  $C$ , on the other hand, is specific to the lattice regularization being used. It is constants of this type which determine the relation between lattice and continuum operators.

$C$  is usually only calculable numerically. To do this the logarithmic divergence has to be subtracted off in some manner. This can be achieved by using a particularly simple class of divergent integrals [21]:

$$\begin{aligned} \mathcal{J}_n(a\kappa) &= \int_{-\pi}^{\pi} \frac{d^4\phi}{(2\pi)^4} \frac{e^{i\phi \cdot n}}{\left[ (a\kappa)^2 + \sum_{\mu} 4 \sin^2 \frac{1}{2} \phi_{\mu} \right]^2} \\ &= \int_0^{\infty} x dx e^{-a^2 \kappa^2 x} e^{-8x} \prod_{\mu} I_{n_{\mu}}(2x), \end{aligned} \tag{A.5}$$

where  $n \in \mathbf{Z}^4$ . The second line uses a modified Bessel function representation (see ref. [22] sect. 8.431) which enables the logarithmic divergence to be isolated and integrated analytically (using the exponential integral function):

$$\mathcal{J}_n(a\kappa) = \frac{1}{(4\pi)^2} \left[ -\ln a^2 \kappa^2 - \gamma_E + F_n \right] + \mathcal{O}(a\kappa). \tag{A.6}$$

Here  $\gamma_E = 0.577216(1)$  is Euler’s constant, and  $F_n$  is a finite integral. Different  $F_n$  can be related to  $F_{0000}$  and  $Z_{0000}$  of eq. (2) using the Bessel function representation. The first few results are

$$\begin{aligned} F_{0000} &= 4.36923(1), \\ F_{1000} &= F_{0000} + (4\pi)^2 \left( -\frac{1}{8} Z_{0000} \right), \\ F_{2000} &= F_{0000} + (4\pi)^2 \left( -\frac{1}{8} - Z_{0000} \right), \\ F_{1100} &= F_{0000} + (4\pi)^2 \left( \frac{1}{48} - \frac{15}{8} Z_{0000} \right). \\ &\vdots \end{aligned} \tag{A.7}$$

In terms of  $\mathcal{J}_n$ , eq. (4) becomes

$$\mathcal{J}(0, a\kappa) = \gamma/2 \mathcal{J}_n(a\kappa) + \lim_{a\kappa \rightarrow 0} \left[ \mathcal{J}(0, a\kappa) + \gamma/2 \mathcal{J}(a\kappa) \right] + \mathcal{O}(a\kappa), \tag{A.8}$$

so that

$$C = -\gamma/2(-\gamma_E + F_n) + \sum_{a\kappa \rightarrow 0} \left[ \mathcal{J}(0, a\kappa) + \gamma/2 \mathcal{J}(a\kappa) \right]. \tag{A.9}$$

The limit in this equation may be taken, and the resulting integral evaluated numerically. In practice an adaptive Monte Carlo multi-dimensional integration package (NAGLIB D01 GBF) was used. This proved sufficiently sophisticated to cope with the integrable singularities present in all of these lattice integrals.

There is an alternative way of calculating logarithmically divergent integrals to the Taylor expansion method outlined above. This is due to Karstan and Smit [23]. The idea is to split the integration region into two parts  $|\phi| < \delta$  and  $|\phi| > \delta$ , so that

$$\mathcal{I}(a\{p\}, a\kappa) = \mathcal{I}_{|\phi| < \delta}(a\{p\}, a\kappa) + \mathcal{I}_{|\phi| > \delta}(a\{p\}, a\kappa).$$

In the inner region ( $|\phi| < \delta$ ) for small  $\delta$  the integrand can be replaced by its continuum value with a spherical cutoff. In the outer region ( $|\phi| > \delta$ ) an expansion in  $a$  is permissible since the integrand is well-behaved, and so the external momentum dependence can be extracted leaving lattice integrals depending only on  $\delta$ .

The specifically lattice contribution to the integral comes from the outer region where the  $\delta \rightarrow 0$  limit is desired. However it is apparent that the inner integral must diverge in this limit ( $\mathcal{I}_{|\phi| < \delta} \sim -(1/(4\pi)^2)\gamma \ln \delta^2$ ), and since  $I$  itself is independent of  $\delta$  there must be a similar divergence in  $\mathcal{I}_{|\phi| > \delta}$ . This divergence can be subtracted off using the exact result

$$\begin{aligned} \mathcal{I}_{|\phi| > \delta} &\equiv \left( \int_{-\pi}^{-\delta} + \int_{\delta}^{\pi} \right) \frac{d^4\phi}{(2\pi)^4} \frac{1}{[\sum_{\mu} 4 \sin^2 \frac{1}{2} \phi_{\mu}]^2} \\ &= -\frac{1}{(4\pi)^2} \ln \delta^2 + \frac{1}{16} K + O(\delta), \end{aligned} \tag{A.10}$$

where  $K = 0.4855321(1)$  [24]. Thus

$$\mathcal{I}_{|\phi| > \delta} = -\gamma/2 \mathcal{I}_{|\phi| > \delta} + \lim_{\delta \rightarrow 0} \left[ \mathcal{I}_{|\phi| > \delta} + \gamma/2 \mathcal{I}_{|\phi| > \delta} \right] + O(\delta).$$

The two approaches are related by the equation

$$\lim_{a\kappa \rightarrow 0} \left[ \mathcal{I}_{0000}(a\kappa) + \frac{1}{(4\pi)^2} (\ln a^2 \kappa^2 + 1) \right] = \lim_{\delta \rightarrow 0} \left[ \mathcal{I}_{|\phi| > \delta} + \frac{1}{(4\pi)^2} \ln \delta^2 \right], \tag{A.11}$$

so that  $\pi^2 K = F_{0000} + 1 - \gamma_E$ .

A third method for extracting divergence has recently been proposed and used by Bernard et al. [18] in their studies of perturbative corrections to four-quark operators in the Wilson formulation.

**References**

- [1] E. de Rafael, Ecole d'été de Physique des Particules, Gif Luminy, Marseille (1983)
- [2] K.G. Wilson, *in* New phenomena in subnuclear physics, ed. A. Zichichi, (Plenum, New York, 1977)
- [3] J. Kogut and L. Susskind, Phys. Rev. D11 (1975) 395
- [4] L. Susskind, Phys. Rev. D16 (1977) 3031
- [5] G. Martinelli and Y.-C. Zhang, Phys. Lett. 123B (1983) 433
- [6] G. Martinelli and Y.-C. Zhang, Phys. Lett. 125B (1983) 77
- [7] S. Sheard, Edinburgh preprint, in preparation
- [8] F.J. Gilman and M.B. Wise, Phys. Rev. D20 (1979) 2392
- [9] M.A. Shifman, A.I. Vainshtein and V.I. Zakharov, Nucl. Phys. B120 (1977) 316
- [10] T.D. Kieu, Edinburgh preprint 1987 388
- [11] D. Daniel and T.D. Kieu, Phys. Lett. 175 (1986) 73
- [12] M.F.L. Golterman and J. Smit, Nucl. Phys. B245 (1984) 61
- [13] D. Verstegen, Nucl. Phys. B249 (1985) 685
- [14] J.E. Mandula, G. Zweig and J. Govaerts, Nucl. Phys. B228 (1983) 91
- [15] G.W. Kilcup and S.R. Sharpe, Nucl. Phys. B283 (1987) 493
- [16] D. Daniel, S. Hands, T.D. Kieu and S.N. Sheard, Phys. Lett. 193B (1987) 85
- [17] G. Altarelli, G. Curci, G. Martinelli and S. Petrarca, Nucl. Phys. B187 (1981) 461
- [18] C. Bernard, A. Soni and T. Draper, UCLA/87/TEP/18 (1987)
- [19] C. Bernard, T. Draper, A. Soni, H.D. Politzer and M.B. Wise, Phys. Rev. D32 (1985) 2343
- [20] C. Bernard, T. Draper, G. Hockney and A. Soni, UCLA/86/TEP/48 (1986)
- [21] A. Gonzalez-Arroyo and C.P. Korthals Altes, Nucl. Phys. B205 [FS5] (1982) 46
- [22] I.S. Gradshteyn and I.M. Ryzhik, Table of integrals, series and products (Academic Press, Orlando, Florida, USA, 1980)
- [23] L.H. Karsten and J. Smit, Nucl. Phys. B183 (1981) 103
- [24] R. Groot, J. Hoek and J. Smit, Nucl. Phys. B237 (1984) 111